

Templated Titania Films with Meso- and Macroporosities

Rutgers University has made this article freely available. Please share how this access benefits you.

Your story matters. <https://rucore.libraries.rutgers.edu/rutgers-lib/42702/story/>

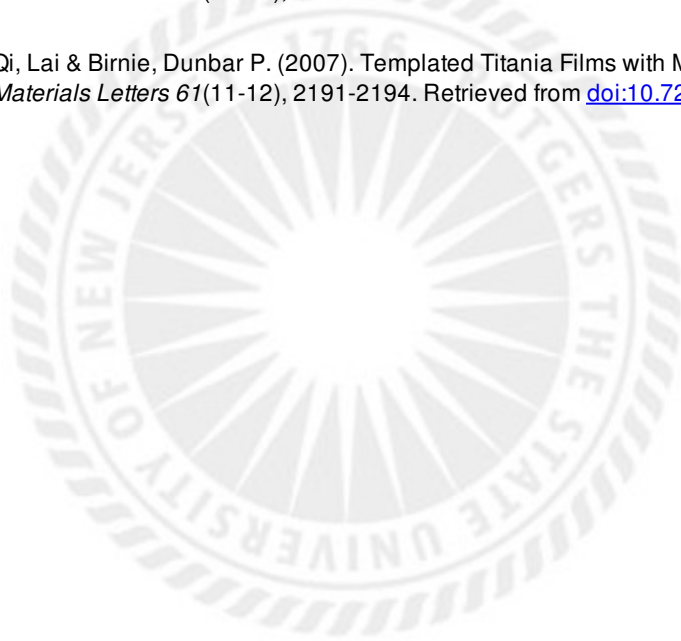
This work is an **ACCEPTED MANUSCRIPT (AM)**

This is the author's manuscript for a work that has been accepted for publication. Changes resulting from the publishing process, such as copyediting, final layout, and pagination, may not be reflected in this document. The publisher takes permanent responsibility for the work. Content and layout follow publisher's submission requirements.

Citation for this version and the definitive version are shown below.

Citation to Publisher Qi, Lai & Birnie, Dunbar P. (2007). Templated Titania Films with Meso- and Macroporosities.
Version: *Materials Letters* 61(11-12), 2191-2194.

Citation to *this* Version: Qi, Lai & Birnie, Dunbar P. (2007). Templated Titania Films with Meso- and Macroporosities.
Materials Letters 61(11-12), 2191-2194. Retrieved from [doi:10.7282/T3S180N4](https://doi.org/10.7282/T3S180N4).



Terms of Use: Copyright for scholarly resources published in RUcore is retained by the copyright holder. By virtue of its appearance in this open access medium, you are free to use this resource, with proper attribution, in educational and other non-commercial settings. Other uses, such as reproduction or republication, may require the permission of the copyright holder.

Article begins on next page

Templated Titania Films with Meso- and Macro- porosities **

Lai Qi, and Dunbar P. Birnie III ^{a)}

Materials Science and Engineering, Rutgers University, Piscataway, NJ 08854, USA

^{a)} Email: dbirnie@rci.rutgers.edu

Abstract

Porous TiO₂ films with both mesoporosity and macroporosity were fabricated by a templated sol-gel method. With incorporation of differently sized pores, the resulted structure is featured of high surface area and an aligned pore network, which are believed to be beneficial for fast charge transportation in electrolytes. The measured specific surface area and porosity of synthesized films were in range of 33-137m²/g and 61-80%, respectively, depending on the size of selected template. Compared to the nanocrystalline films widely applied in current dye-sensitized solar cells (DSC), the reported structure has additional feature facilitating electrolyte diffusion and provides possible approaches towards efficient all-solid-state or quasi-solid-state junctions.

Dye-sensitized solar cells (DSC) that adopt porous TiO₂ film as the photoelectrode demonstrate high solar conversion efficiencies (over 10%) at competitively low costs.¹⁻⁴ Under illumination, the photon excited electron-hole pairs disassociate at the interface between TiO₂ and adsorbed sensitizers (dye). Free electrons are injected from sensitizers into the conduction band of TiO₂; while the holes are conveyed away to the counter electrode by electron transfer from electrolyte to the oxidized sensitizers and subsequently electrolyte diffusion.² Decided by this operation mechanism, an ideal TiO₂ electrode is believed to possess a large surface area accessible to both dye molecules and redox species in the electrolyte. By interpenetrating a pore

network into a TiO₂ network, it provides pathways for both charges towards opposite electrodes after their separation. Optimal efficiency is due to balanced charge transportation ability in both ways.

Currently, doctor-blade method^{1,5} and screen printing⁶ are the most frequently used techniques to prepare nanocrystalline TiO₂ films for DSC, a process similar to the prototype DSC developed in 1991.¹ After depositing a layer of 5-50nm nanoparticles and a brief sintering at 400-500°C, porous nanocrystalline films result due to random packing of particles. The average pore size usually falls in the same range of the particle size. Though this mesoporosity (usually 50-60%) may offer a strikingly high internal surface area (e.g. a roughness factor of 460/μm),⁷ the influence of the randomly tortuous and narrowed pore channels on the diffusion rate of electrolyte is believed to be negative. As pointed out by Grätzel,^{6,7} a desired TiO₂ structure should possess a high degree of order with mesoporous channels aligned in parallel to each other and perpendicular to the electrode substrate.

Templated growth combined with sol-gel coating technique provides approaches to fabricate fine nanostructure of desired features.^{8,9,15-22} Jiu and Adachi⁹ reported templated growth of porous TiO₂ films with mixed templates of Pluronic F-127 and cetyltrimethylammonium bromide. Zúkalová⁸ reported a similar structure with Pluronic P-123. Both works achieved very high surface areas but with quite small pore diameters, 4-7nm⁹ and 6-8nm,⁸ respectively. For the concerns of mass transportation in TiO₂¹⁰ and embodiment of all-solid-state or quasi-solid-state DSC, decreased pore size may present difficulties for complete coating of sensitizers (due to the relatively large molecule size of the Ruthenium based sensitizers¹¹), the diffusion of redox species, and infiltration of organic hole conductor.¹² Somani¹³ and Huisman¹⁴ reported an inverse opal (IO) TiO₂

structure for DSC, which were composed of macropores prepared by an assemble-infiltration process. Somani¹³ reported a superior performance of this IO TiO₂ structure in a solid-state DSC than the traditional nanocrystalline.

Inverse opal of TiO₂ or other materials have been reported previously¹⁵⁻²² by a template-infiltration two-step process. The template particles were assembled first; then a metal organic precursor solution was infiltrated by the capillary effect. Because organic metal compounds suffer large volume shrinkage during decomposing to oxides, cracking is inevitable and a complete filling of the template by single infiltration is difficult. Repeated infiltration is necessary, which alone may take days²⁰ or even weeks.¹⁷

In this communication, we report a simply mixing-casting method for templated TiO₂ structures with improved film uniformity, less cracking and easier process from

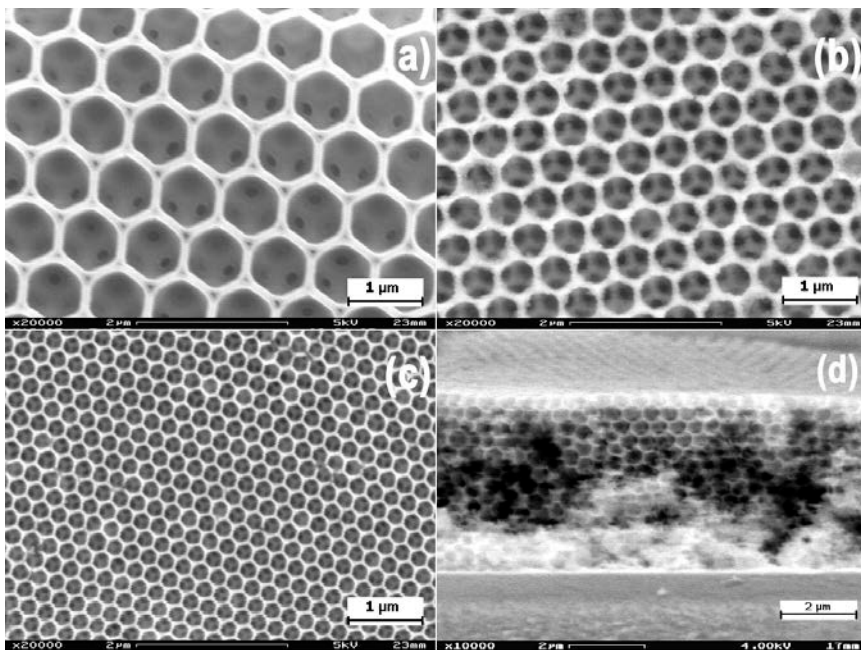


Figure 1. SEM micrographs of TiO₂ films derived from sol-gel precursor with differently sized templates. (a) 1 μm; (b) 600nm; (c) 300nm; (d) Cross view of the 600nm. The coating method was cast-coating after mixing the precursor solution and PS template solution by ultrasonication for 2 minutes.

previously reported IO structures.^{13,14} The preparation is also based on self-assembly of polystyrene (PS) spheres coupled with either TiO₂ sol-gel precursor or pre-synthesized TiO₂ nanocrystals (Degussa, P25, ~50nm). The developed structures show an aligned macropore network interpenetrating into a nanocrystalline film, which is capable to improve charge transport capability without significantly lowering the surface area.

Figure 1 shows the scanning electron microscope (SEM) micrographs of the synthesized porous TiO₂ from TiO₂ sol-gel precursor. The colorless and transparent sol-gel precursor was prepared by hydrolysis of titanium tetra-isopropoxide (Aldrich, 98%), and then redissolving in a certain amount of concentrated HCl. The chemical composition is similar to that of those prepared by reacting TiCl₄ with ice.²³ From the top views (Figure 1a-c), it can be seen that the TiO₂ forms a three dimensionally honeycomb-like network with an interpenetrated network of closely packed air spheres. All the pores are spatially aligned and interconnected with an average size slightly smaller than the size of PS templates. The pore size of synthesized TiO₂ porous films can be controlled by adopting differently sized templates with average pore size varying from 1 μ m to 300nm.

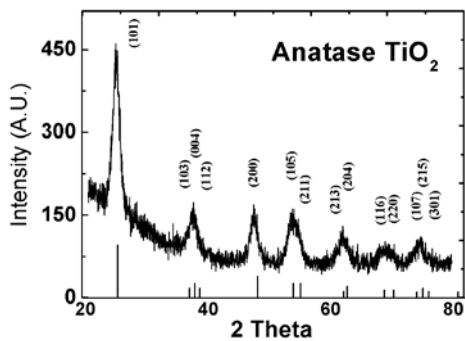


Figure 2. X-ray diffraction pattern of the sol-gel derived porous TiO₂. The lines are known anatase TiO₂ (JCPDS# 21-1272).

The cross-section view of the TiO₂ film is shown in Figure 1d. It can be observed that most of the pores in the top layers are self-assembled into a face-centered-cubic structure (A-B-C-A stacking), which is consistent with the top view observation. The pore arrangement in the lower part of the layer is suspected to have lower regularity than that of the upper part, possibly due to the substrate confinement. But all the pores are closely or nearly closely packed.

The X-ray diffraction (XRD) pattern of prepared porous TiO₂ film is shown in Figure 2. After annealing at 400°C for 1 hour, pure anatase phase was obtained without observation of other phases. Varying the particle size of the template changes the specific surface area (the roughness factor), pore size and porosity of the resulted films. These factors are important for applications, such as DSC, fuel cells, electrochemical batteries, sensors and catalysts. Table 1 lists the specific surface area (S_A) and porosity (P_r) data of the TiO₂ films with different template sizes measured by the Brunauer-Emmett-Teller (BET) method. The samples were powders scratched off from their substrates. With size decreasing from 1 μ m to 160nm, the specific surface area increases from 33.2m²/g to 137.2m²/g. The roughness factor (R_f) is calculated by: $R_f = 4.2 \times (1 - P_r) \times S_A$, where 4.2 is the density of fully crystallized anatase with the unit of g/cm³. The porosities of films with 300nm and 600nm pore size are higher than 70%.

Table 1. Specific surface area and porosity data of the synthesized TiO₂ films.

Ave. pore size (nm)	Brunauer-Emmett-Teller (BET)		
	Spec. surf. area (m ² /g)	Roughness factor (μ m ⁻¹)	Porosity (%)
1000	33.2	53.7	61.5
600	60.1	69.7	71
300	119.1	148.1	70.4
160	137.2	197.1	65.8

Another advantage for the large pore size of this honeycomb TiO_2 is its potential to work with polymer electrolytes to form an all-solid-state junctions,^{2,24} because polymer electrolytes usually have high viscosity and large molecular size, and thus, are difficult to be filled into tiny pores. We reproduced the honeycomb TiO_2 structure with pre-synthesized TiO_2 nanocrystals. Figure 3 shows SEM micrographs of porous TiO_2 films of P25 nanoparticles templated by $1\mu\text{m}$ PS nanospheres. With the P25 precursor, we observed very few cracking as shown in Figure 3a, which might be due to the negligible shrinkage of the P25 particles during heating. At high magnification (Figure 3b,c), individual P25 particles and the mesoporosity between them become distinguishable. The rest space inside the film forms an interpenetrating and aligned macropore network. Mercury porosimetry (Micromeritics, Autopore III) was adopted to investigate the pore size distribution, which is shown in Figure 4. Without templating, P25 formed

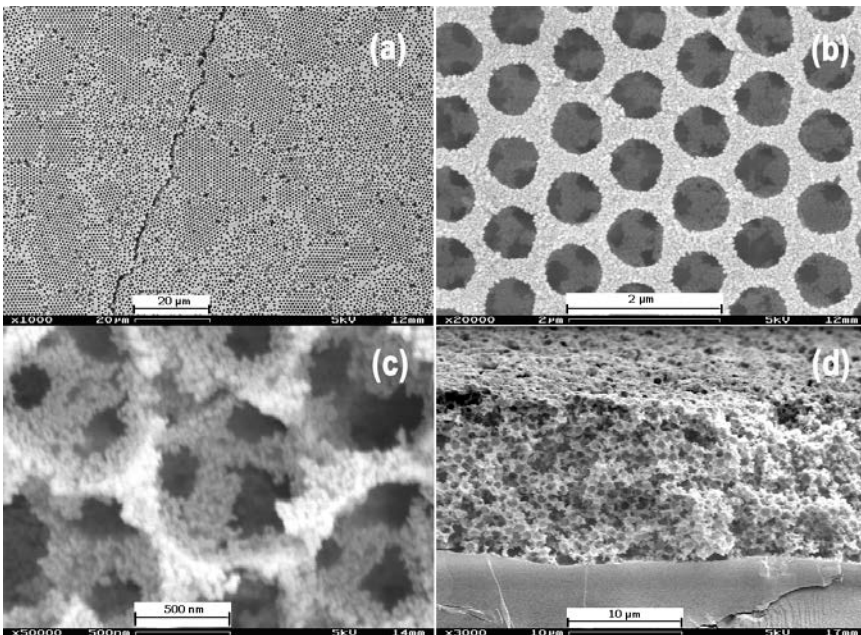


Figure 3. SEM micrographs of porous P25 films with both macro- and meso- porosities templated by $1\mu\text{m}$ PS at different magnifications (a) $1000\times$, (b) $20,000\times$, (c) $50,000\times$, (d) Cross view of a $15\mu\text{m}$ thick film.

film with an average pore size of 32nm and very narrow pore sized distribution. Templated with 1 μ m PS, double peaks appear in the pore volume – pore size diagram, which are centered at 35nm and 520nm, respectively. The first peak indicates preserved mesoporosity; while, the second peak proves the existence of macroporosity due to templates. The obvious size reduction of pores (530nm) from their template (1 μ m) is possibly due to two reasons. First, films shrink during annealing, which reduces the pore size by about 20%. Second, mercury intrusion records actually the size of pore opening, which is smaller than the pore diameter in this case.

In traditional nanocrystalline films prepared by the doctor-blade method,¹⁻⁶ the pore spaces are typically tightly constricted and some fraction of closed pore volume is inevitable, which lowers the actual surface area accessible to dyes. In the honeycomb TiO₂ films of this work, the large pore size and aligned pore channels make the inner surface more accessible to dyes and redox species. Considering the big size of organic

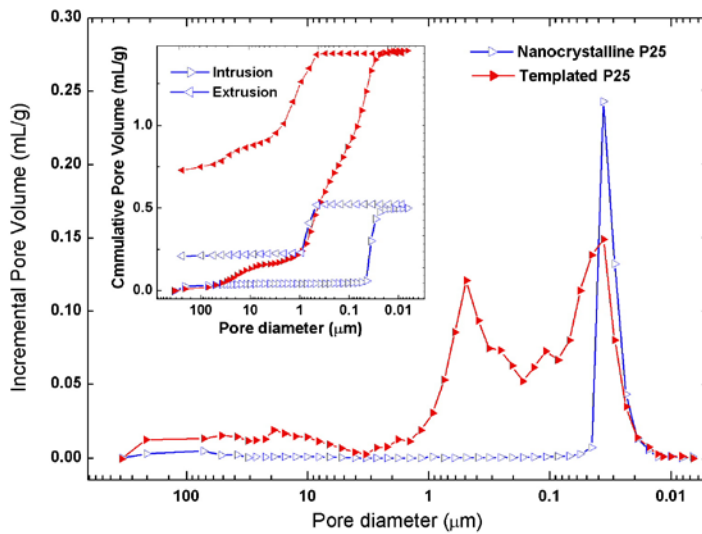


Figure 4. Pore size distribution of templated P25 films by mercury porosimetry. (Open triangle: non-templated P25; solid triangle: P25 templated with 1 μ m PS). Inset: the isotherms of both films.

hole conductors,¹² this templated P25 films show higher potential than mesoporous nanocrystalline films towards efficient all-solid-state or quasi-solid-state junctions.

We report a simple method for preparation of TiO₂ films with both meso- and macro-porosity. The prepared films contain aligned and closely packed pore networks. Not only high porosity, large pore size and high surface area could be achieved together, but also the flexibility to customize those parameters makes the synthesized materials promising for some applications.

Reference

1. B. O'Regan, and M. Grätzel: A low-cost, high-efficiency solar cell based on dye-sensitized colloidal TiO₂. *Nature* **353**, 737 (1991).
2. U. Bach, D. Lupo, P. Comte, J. E. Moser, F. Weissortel, J. Salbeck, H. Spreitzer, and M. Gratzel: Solid-state dye-sensitized mesoporous TiO₂ solar cells with high photon-to-electron conversion efficiencies. *Nature*, **395**, 583 (1998).
3. Jinting Jiu, Fumin Wang, Masaru Sakamoto, Jun Takao, and Motonari Adachi: Preparation of Nanocrystalline TiO₂ with Mixed Template and Its Application for Dye-Sensitized Solar Cells. *J. Electrochem. Soc.*, **151**, A1653 (2004).
4. N. Kopidakis, K. D. Benkstein, J. van de Lagemaat, and A. J. Frank: Transport-Limited Recombination of Photocarriers in Dye-Sensitized Nanocrystalline TiO₂ Solar Cells. *J. Phys. Chem. B* **107**, 11307 (2003).
5. M. Adachi, Y. Murata, J. Takao, J. Jiu, M. Sakamoto, F. Wang, *J. Am. Chem. Soc.* **2004**, *126*, 14943.
6. M. Grätzel: Perspectives for Dye-sensitized Nanocrystalline Solar Cells. *Prog. Photovolt Res. App.* **8**, 171 (2000).
7. M. Grätzel: Dye-sensitized solar cells. *J. Photochem. Photobio. C: Photochem. Rev.*, **4**, 145 (2003).

8. M. Zikalova, A. Zikal, L. Kavan, M. K. Nazeeruddin, P. Liska, and M. Grätzel: Organized Mesoporous TiO₂ Films Exhibiting Greatly Enhanced Performance in Dye-Sensitized Solar Cells. *Nano Lett.*, **5**, 1789 (2005).
9. J. Jiu, F. Wang, M. Sakamoto, J. Takao, and M. Adachi: Performance of dye-sensitized solar cell based on nanocrystals TiO₂ film prepared with mixed template method. *Solar Energy Mater. & Solar Cells*, **87**, 77 (2005).
10. K. D. Benkstein, N. Kopidakis, J. van de Lagemaat, and A. J. Frank: Influence of the Percolation Network Geometry on Electron Transport in Dye-Sensitized Titanium Dioxide Solar Cells. *J. Phys. Chem. B*, **107**, 7759 (2003).
11. M. Grätzel: Nanocrystalline Solar Cells. *Renewable Energy*, **5**, 118 (1994).
12. U. Bach, Y. Tachibana, J. Moser, S. A. Haque, J. R. Durrant, M. Gratzel, and D. R. Klug: Charge Separation in Solid-State Dye-Sensitized Heterojunction Solar Cells. *J. Am. Chem. Soc.* **121**, 7445 (1999).
13. P. R. Somani, C. Dionigi, M. Murgia, D. Palles, P. Nozar, and G. Ruani: Solid-state dye PV cells using inverse opal TiO₂ films. *Solar Energy Mater. Solar Cells*, **87**, 513 (2005).
14. C. L. Huisman, J. Schoonman, and A. Goossens: The application of inverse titania opals in nanostructured solar cells. *Solar Energy Mater. & Solar Cells*, **85**, 115 (2005).
15. J. E. G. J. Wijnhoven, and W. L. Vos: Preparation of Photonic Crystals Made of Air Spheres in Titania. *Science*, **281**, 802 (1998).
16. P. Jiang, J. Cizeron, J. F. Bertone, and V. L. Colvin: Template-directed preparation of macroporous polymers with oriented and crystalline arrays of voids. *J. Am. Chem. Soc.*, **121**, 7957 (1999).
17. P. Ni, B. Cheng, and D. Zhang: Inverse opal with an ultraviolet photonic gap. *Appl. Phys. Lett.*, **80**, 1879 (2002).
18. B. T. Holland, C. F. Blanford, and A. Stein: Synthesis of Macroporous Minerals with Highly Ordered Three-Dimensional Arrays of Spheroidal Voids. *Science*, **281**, 538 (1998).
19. M. E. Abdelsalam, P. N. Bartlett, J. J. Baumberg, and S. Coyle: Preparation of arrays of isolated spherical cavities by self-assembly of polystyrene spheres on self-assembled pre-patterned macroporous films. *Adv. Mater.* **16**, 90 (2004).

20. Z. Zhong, Y. Yin, B. Gates, and Y. Xia: Preparation of mesoscale hollow spheres of TiO₂ and SnO₂ by templating against crystalline arrays of polystyrene beads. *Adv. Mater.*, **12**, 206 (2000).
21. A. Richel, N. P. Johnso, and D.W. McComb: Observation of Bragg reflection in photonic crystals synthesized from air spheres in a titania matrix. *Appl. Phys. Lett.*, **76**, 1816 (2000).
22. Z. Zhou, and X. S. Zhao: Opal and inverse opal fabricated with a flow-controlled vertical deposition method. *Langmuir*, **21**, 4717 (2050).
23. M. K. Nazeeruddin, P. Pe'chy, T. Renouard, S. M. Zakeeruddin, R. Humphry-Baker, P. Comte, P. Liska, L. Cevey, E. Costa, V. Shklover, L. Spiccia, G. B. Deacon, C. A. Bignozzi, and M. Gra'tzel: Engineering of Efficient Panchromatic Sensitizers for Nanocrystalline TiO₂-Based Solar Cells. *J. Am. Chem. Soc.*, **123**, 1613 (2001).
24. P. Wang, S. M. Zakeeruddin, J. E. Moser, M. K. Nazeeruddin, T. Sekiguchi, M. Grätzel: A stable quasi-solid-state dye-sensitized solar cell with an amphiphilic ruthenium sensitizer and polymer gel electrolyte. *Nature Mater.*, **2**, 402 (2003).